Ethynyl-Tolyl Extended 2-(2'-Hydroxyphenyl)benzoxazole Dyes: Solution and Solid-state Excited-State Intramolecular Proton Transfer (ESIPT) Emitters

Maxime Munch, Mathieu Curtil, Pauline Vérité, Denis Jacquemin, Julien Massue, Gilles Ulrich

Ethynyl-Tolyl Extended 2-(2'-Hydroxyphenyl)benzoxazole Dyes: Solution and Solid-state Excited-State Intramolecular Proton Transfer (ESIPT) Emitters

Maxime Munch,[a] Mathieu Curtil,[a] Pauline M. Vérité,[b] Denis Jacquemin,[b*] Julien Massue,[a*] and Gilles Ulrich[a*]

Abstract: Dual solution/solid-state emissive fluorophores based on a 2-(2'-Hydroxyphenyl)benzoxazole (HBO) core bearing one or two ethynyl-tolyl moieties at different positions were synthesized *via* an expedite two-step synthetic procedure. HBO derivatives are known to display intense Excited-State Intramolecular Proton Transfer (ESIPT) emission in the solid-state but are mildly emissive in solution due to the detrimental flexibility of the excited-state opening efficient non-radiative pathways. The sole introduction of a rigid ethynyl moiety led to a sizeable enhancement of the fluorescence quantum yield in solution, up to a 15-fold increase in toluene as compared to unsubstituted HBO dyes while keeping the high solid-state fluorescence efficiency. The position of the substitution on the π-conjugated core led to subtle fine-tuning of maximum emission wavelengths and quantum yields. Moreover, we show that the ethynyl tolyl substituent at the para position of the phenol ring is a suitable moiety for an efficient stabilization of the corresponding emissive anionic HBO derivatives in dissociative solvents like DMF THF or EtOH. These observations were confirmed in CH_3CN by a basic titration. For all dyes, the nature of the excited-state involved in the fluorescence emission was rationalized using *ab initio* calculations.

Introduction

Photoinduced proton transfer is one of the most important chemical reactions in nature and plays a pivotal role in a wide range of biological processes.[1] Depending on environmental dynamics, proton transfer can occur in many different ways; therefore, understanding and controlling such processes is of upmost importance not only for academic purposes but also to target valuable applications. Excited-State Intramolecular Proton Transfer (ESIPT) processes consist of a photoinduced proton transfer occurring within a molecular entity. Consequently, ESIPT leads to the presence of different tautomers in the ground and excited-state which induces large Stokes shifts, *i.e.* a strong spectral separation between absorption and emission bands.[2] ESIPT was first evidenced in natural heterocyclic structures[3] and further extended to synthetic chromophores, including notably 2-(2'-hydroxyphenyl)benzazole (HBX) derivatives[4] as well as many others.[5] While the range of organic structures prone to display ESIPT is wide, a common feature to all ESIPT dyes lies in the presence of a strong intramolecular H-bond. which can involve various donors and acceptors and form five, six, seven or eight-membered rings.[6] Many structural and environmental parameters can impact the H-bond energy and thus the ESIPT process efficiency, leading to single or dual emitters, depending on the strength and nature of the H-bond.[7] Additionally, physical factors such as temperature, viscosity, pH or polarity/proticity in the close vicinity of the dye have a strong impact on both the position and intensity ratio of the tautomeric emission bands.[8] As a consequence, each ESIPT dye displays a unique, characteristic environment-sensitive emission pattern which has been beneficially utilized in various areas where the microenvironment is prone to undergo subtle changes, such as cellular imaging[9] or fluorescence sensing.[10] ESIPT luminescence is however rather faint in solution, owing to detrimental motions occurring in the excited-state, triggering efficient non-radiative pathways and consequently leading to a strong quenching of fluorescence radiations. A trademark of ESIPT probes is their typical solid-state brightening due to a beneficial restriction of molecular torsions which contributes to a significant decrease of non-radiative deactivations.[11] The engineering of ESIPT dyes displaying fluorescence emission both in solution and in the solid-state still appear as a serendipitous challenge.[12] In this article, we demonstrate that the sole introduction of ethynyl tolyl substituents at the periphery of 2-(2'-hydroxyphenyl) benzoxazole (HBO) dyes is sufficient to reach a significant enhancement of quantum yield (Φ_F) in the solution-state (multiple solvents were considered) while maintaining a strong fluorescence intensity in the solid-state. Furthermore, we show that the extension of conjugation *via* a triple bond at the 5 position of the phenol ring leads to the stabilization of an emissive anionic species in dissociative solvents or upon addition of a base in CH_3CN. The general structure of the dyes studied is presented on Figure 1. All these observations are rationalized using *ab initio* calculations.

[a] Maxime Munch, Mathieu Curtil, Dr. Julien Massue, Dr. Gilles Ulrich
Institut de Chimie et Procédés pour l'Energie, l'Environnement et la Santé (ICPEES), UMR CNRS 7515, Ecole Européenne de Chimie, Polymères et Matériaux (ECPM), 25 Rue Becquerel, 67087 Strasbourg Cedex 02, France
E-mail: massue@unistra.fr, gulrich@unistra.fr
[b] Pauline M. Vérité, Prof. Dr. Denis Jacquemin,
CEISAM, UMR CNRS 6230, BP 92208, 2 rue de la Houssinière, 44322 Nantes, Cedex 03, France
E-mail: Denis.Jacquemin@univ-nantes.fr

Supporting information for this article is given via a link at the end of the document.

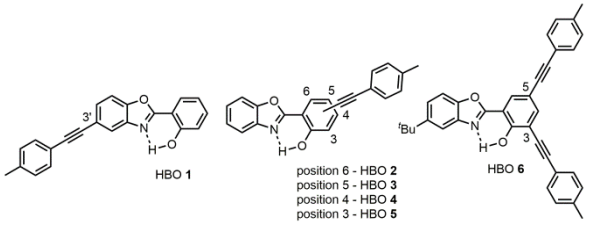

Figure 1. General structure of the ESIPT emitters HBO **1-6.**

Results and Discussion

The synthesis of HBO dyes **1-2** and **5-6** is described on Schemes 1 to 4 while the structure of reported HBO dyes **3**[13] and **4**[13] is presented on Figure 2.

The synthesis of HBO dyes **1-6** is very straightforward, consisting of two synthetic steps starting from commercially available reagents. The HBO core was constructed *via* two alternative routes depending on substitution. HBO **7** and **10** bearing a bromine atom were formed by reacting the appropriate 2-aminophenol and salicylaldehyde derivatives in the presence of an excess of phenylboronic acid and potassium cyanide in methanol at room temperature. HBO **9** and **11** bearing iodine atoms were formed by refluxing the corresponding reagents in ethanol followed by oxidation at room temperature in dichloromethane with a slight excess of 2,3-dichloro-5,6-dicyano-1,4-benzoquinone (DDQ). It is necessary to protect the phenol ring in HBO **10** and **11** with an acetate group in order to avoid Pd-catalyzed intramolecular cyclization leading to the formation of an undesired benzofuran derivative.[14] Sonogashira cross-coupling reactions on the halogenated intermediates **7** and **9**-**11** were performed in a mixture of toluene and triethylamine using a catalytic amount of Pd(II) catalyst, either $PdCl_2(PPh_3)_2$ or $Pd(dppf)Cl_2$ and copper iodide to afford the target HBO dyes **1-2** and **5-6** after purification by column chromatography on silica gel. All compounds were characterized by ^1H and ^{13}C NMR spectroscopy, HR-MS and FT-IR (see the experimental section and Supporting Information, ESI).

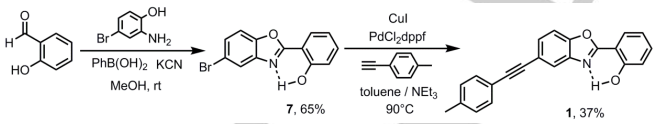

Scheme 1. Synthesis of HBO **1.**

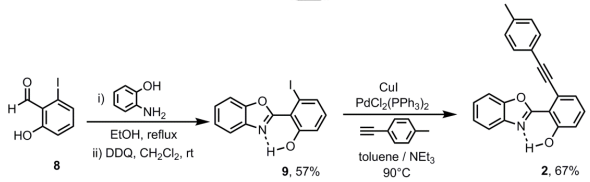

Scheme 2. Synthesis of HBO **2**.

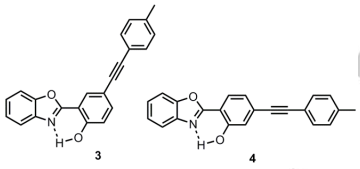

Figure 2. Structure of dyes **3** and **4**.[13]

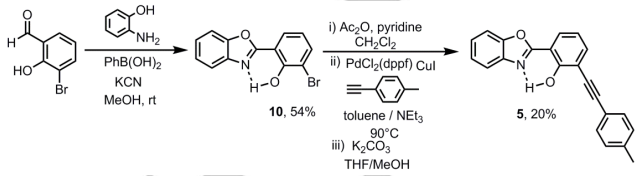

Scheme 3. Synthesis of HBO **5.**

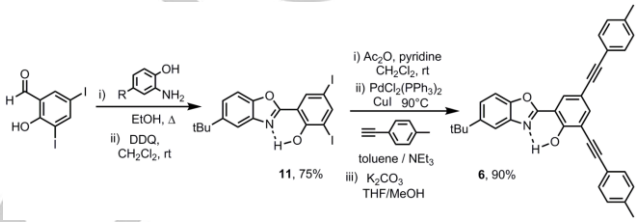

Scheme 4. Synthesis of HBO **6.**

The photophysical properties of HBO 1-6 measured in solution and in the solid-state are gathered in Table 1. The absorption and emission spectra of all dyes in solution are respectively presented in Figures 3a and 3b while absorption and emission spectra of HBO dye **6** in a range of solvents are respectively depicted in Figures 4a and 4b. Full list of spectral data can be found in the ESI.

The absorption spectra of HBO derivatives **1-6** in toluene feature similar trends such as a broad, rather unstructured band assigned to the S_0-S_1 transition, with a maximum wavelength comprised between 332 and 368 nm. The additional absorption bands observed at higher energies (below 300 nm) are assigned to the π-π* transitions of the phenyl rings. Molar absorption coefficients are in the 15000 to 45000 $M^{-1}.cm^{-1}$ range, which is typical for compact polyaromatic dyes (Figure 3a). The absorption spectra in ethanol display very similar features as those observed in toluene (see the SI), which indicates that the optical properties in the ground state are not strongly influenced by the substitution pattern nor the nature (dipolarity) of the solvent.

Upon excitation in the lowest-energy absorption band in toluene (λ_{exc} = 330-350 nm), all HBO dyes **1-6** display a single intense emission band whose maximum wavelength spans from 489 to 550 nm depending on the position of the ethynyl tolyl substituent(s) on the HBO core. In all cases, the excitation spectrum matches well the absorption one, excluding the presence of emissive aggregates in the excited-state (see the SI). The Stokes' shifts (SS) are in the range 8000-11000 cm^{-1} which is typical of ESIPT emitters. These SS values, larger than in standard organic fluorophores, are consistent with the formation of the keto tautomer in the excited-state (K*), as a consequence of the phototautomerization process.

Table 1. Optical data of HBO dyes **1-6** and **12** measured in aerated solution at room temperature or dispersed in potassium bromide pellets.

Dye	λ_{abs} (nm)	ε ($M^{-1}.cm^{-1}$)	λ_{em} (nm)	SS[b] (cm^{-1})	Φ_F [c]	τ(ns)[d]	K_r ($10^8 s^{-1}$)[e]	K_{nr} ($10^8 s^{-1}$)[e]	
1	332	30200	504	10000	0.04	2.1	0.20	4.80	toluene
1	329	28400	398/489	5300	0.02	3.3	0.06	2.97	EtOH
1	362	-	489	7200	0.88	-	-	-	solid[f]
2	332	27000	519	11000	0.23	3.2	0.72	2.41	toluene
2	328	11000	402/508	5600	0.20	0.5/1.2	1.67	6.67	EtOH
2	355	-	503	8300	0.68	-	-	-	solid[f]
3	347	37200	397/514	3600	0.10	1.3	0.77	6.92	toluene
3	341	10200	398/511	4200	0.07	1.1	0.64	8.45	CH_2Cl_2
3	345	11400	404/444/512	4200	0.04	0.5/3.2	0.80	19.20	THF
3	338	12200	399/511	4500	0.03	0.4/2.8	0.75	24.30	CH_3CN
3	345	11500	389/450/505	3300	0.04	0.5/3.1	0.23	5.55	EtOH
3	351	15000	384/465[a]	2400	-	-	-	-	DMF
	417	4100	467[a]	2600	-	-	-	-	DMF
3	368	-	530	8300	0.51	-	-	-	solid[f]
4	349	45700	489	8200	0.19	1.8	1.06	4.50	toluene
4	345	28800	398/485	3900	0.16	1.4	1.14	6.00	EtOH
4	370	-	504	7200	0.63	-	-	-	solid[f]
5	349	19000	550	10000	0.32	2.3	1.39	2.96	toluene
5	342	19000	538	10100	0.17	1.6	1.06	5.19	EtOH
5	368	-	504	7300	0.60	-	-	-	solid[f]
6	368	15600	550	9000	0.30	3.4	0.85	2.09	toluene
6	375	16000	550	8500	0.35	3.7	0.95	1.76	CH_2Cl_2
6	375	14600	470/550	5400	0.21	3.1	0.68	2.55	THF
6	365	15600	474/545	6300	0.30	3.5	0.86	2.00	CH_3CN
6	371	14700	540	8400	0.24	3.2	0.75	2.38	EtOH
6	361	30600	388/495	1000	0.23	3.3/3.5	0.68	2.26	DMF
	460	21100	495	1500	0.49	3.3/3.5	0.14	0.15	DMF
6	388	-	547	7500	0.48	-	-	-	solid[f]
12	321	23100	406/490	6500	0.02	3.6	0.06	2.72	toluene
12	317	20800	397/481	6400	0.01	2.8	0.04	35.4	EtOH

[a] A poor match was observed between absorption and excitation spectra evidencing the formation of aggregates in the excited-state, hence the impossibility to accurately calculate the fluorescence quantum yield of the molecular species.

[b] Stokes' shift

[c] Quantum yield determined in solution by using Rhodamine 6G as a reference (λ_{exc} = 488 nm, Φ = 0.88 in ethanol) or as an absolute value using a spectrofluorimeter fitted with an integration sphere.

[d] Fluorescence lifetime

[e] k_r (10^8 s^{-1}) and k_{nr} (10^8 s^{-1}) were calculated using the following equations: $k_r = \Phi_F/\tau$, $k_{nr} = (1- \Phi_F)/\tau$.

[f] Embedded in potassium bromide pellet. Concentration around 10^{-4} M.

In the case of HBO **3**, a very small shoulder can be observed in the higher energies (λ_{em} = 397 nm) which can be assigned to the residual presence of the enol tautomer (E^*) in the excited-state, evidencing a partially frustrated ESIPT process. The E^* band is indeed characterized by a smaller SS, consistent with a significantly least reorganization of the molecular structure in the excited-state. As can be observed in Figure 3b, the position of the ethynyl tolyl fragment on the HBO core has a subtle but non negligible influence on the maximum emission wavelength. HBO **4**, bearing a substituent at the 4 position of the phenol ring presents the most blue-shifted emission of the series (λ_{em} = 489 nm); an observation consistent with a weakly polarized excited-state. HBO **1,2** and **3** with a respective substitution at the 3', 6 and 5 position of the HBO scaffold display similar maximum emission wavelengths at 504, 519 and 514 nm respectively. HBO **5** and **6** which share a common substitution at position 3 of the HBO core are the most bathochromically shifted in the series (λ_{em} = 550 nm), highlighting the beneficial impact of the ethynyl tolyl fragment at the *ortho* position of the phenol ring for a red-shifted emission. This can be also indicative of the presence of a weak but sizeable internal charge transfer (ICT) state in these dyes.

The most striking influence of the position of the functionalization on the optical properties of HBO dyes **1-6** lies in the fluorescence quantum yield values in solution. As listed in Table 1 and schematically represented on Figure 3c, drastic differences can be observed in the isomers series. As a general observation, the introduction of a single ethynyl tolyl group on the phenol ring leads to a strong enhancement of Φ_F as compared to unsubstituted HBO derivatives, with values ranging from 10 to 32% in toluene. As a reference, 4-methyl-2-(2'-hydroxyphenyl)benzoxazole **12**, bearing a methyl group at the 4 position was synthesized[15] and its optical properties investigated in toluene and ethanol (Table 1 and Figure 4).

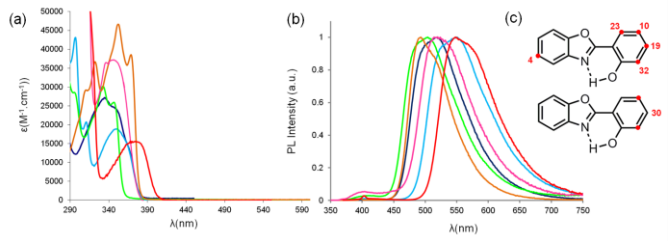

Figure 3. (a) Absorption spectra, (b) Emission spectra recorded in toluene at room temperature for HBO **1** (green), HBO **2** (navy blue), HBO **3** (pink), HBO **4** (light blue), HBO **5** (pink) and HBO **6** (red) and (c) Schematic representation of the value of the fluorescence quantum yield in toluene for each substitution position.

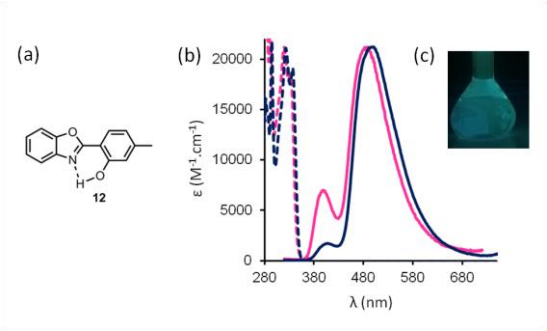

Figure 4. (a) Structure of HBO **12**, (b) UV-Visible (dashed) and emission (plain) spectra of HBO **12** in toluene (navy blue) and ethanol (pink) and (c) Photograph of HBO dye **12** in solution in toluene under irradiation by a bench UV lamp (λ_{exc} = 365 nm).

HBO **12** displays blue-shifted absorption and emission spectra compared to HBO dyes **1-6** ($\lambda_{abs}/\lambda_{em}$ = 321/406-490 nm and 317/397-481 nm for **12** in toluene and ethanol respectively). HBO **12** is barely emissive in solution, as shown of Figure 4c (Φ_F = 2% in toluene and Φ_F = 1% in ethanol, leading to K_r/K_{nr} values of 0.06/2.72 and 0.04/3.54 10^8 s^{-1} in these two solvents).

HBO **5** and **6** which include a single or a double ethynyl tolyl substitution at position 3 and/or 5 are the most emissive dyes in the series with quantum yields reaching 32 and 30% in toluene, respectively; a 16/15-fold enhancement with respect to unsubstituted HBO **12**. HBO **1**, the only dye in the series substituted on the benzoxazole side stand out as weakly emissive (Φ_F = 4% in toluene), further highlighting the beneficial role of the substitution on the phenol ring to gain fluorescence intensity. This luminescence enhancement is correlated with a strong increase of the radiative constant values (K_r = 0.06, 0.85 and 1.39 10^8 s^{-1} for HBO **12**, **6** and **5**, respectively). The non-radiative constant rates along with the fluorescent lifetimes remain however in the same range regardless of substitution (K_{nr} = 2.72, 2.09 and 2.96 10^8 s^{-1}, τ = 3.6, 3.4 and 2.3 ns for HBO **12**, **6** and **5**, respectively). We wish to underline that these purely organic solution-state emissive ESIPT emitters can be obtained in only two or three synthetic steps from commercially available starting materials, allowing a facile synthesis on a multigram scale in the laboratory. Moreover, it is worth mentioning that these results highlight the interest of using oxygen-based rather than sulfur-based heterocycles, the latter more efficiently leading to intersystem crossing and, consequently smaller Φ_F.[16] Triple bond extended conjugation on the phenol ring, along with the presence of a benzoxazole scaffold seem to be of paramount importance in order to reach improved luminescence intensity in solution. Moreover, the substitution at the specific 3 position of the HBO core, *i.e.* adjacent to the hydroxy group leads to the largest quantum yield in the series. In ethanol, all dyes with the notable exception of **5** and **6** display a dual E*/K* emission, as a result of the stabilization of the enol tautomer (E*) in the excited-state owing to the formation of intermolecular H-bonds. Interestingly, the present dyes remain emissive in ethanol (Φ_F = 17 and 24% respectively), whereas protic environments are known to often quench ESIPT emission.[17]

Dye **3** stands out by the presence of an additional emission band at 450 nm in ethanol (Figure S3.6) which is reminiscent of what was observed for reported HBO derivatives featuring a highly acidic phenolic proton where the deprotonated conjugated base D* was found to be both stable and emissive.[18] With an extended conjugation at the para position of the hydroxy group, HBO dye **3** displays a triple E*/D*/K* emission behavior with, however a quenching of the fluorescence (Φ_F = 4% in ethanol). It is interesting to note that this triple emission is not observed in dye **6** in ethanol which also presents a para substitution. In order to shed more light on the photophysical properties of these para-substituted dyes, the optical behavior of HBO dyes **3** and **6** were studied in a range of solvents of different dipolarity and proticity (Figures S3.4-S3.7 and Figure 5, respectively).

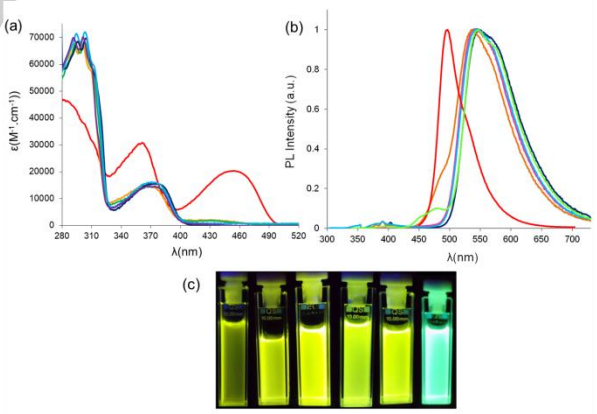

Figure 5. (a) Absorption spectra and (b) emission spectra of HBO **6**, recorded at room temperature in aerated solutions of toluene (navy blue), dichloromethane (light blue), THF (green), acetonitrile (orange), ethanol (purple) and DMF (red) and (c) Photographs of HBO **6** under irradiation with a bench UV lamp (λ_{exc} = 365 nm) in toluene, dichloromethane, THF, acetonitrile, ethanol and DMF (from left to right).

For HBO dye **3**, the maximum absorption wavelength is not very sensitive to the nature of the solvent (λ_{abs} = 338-351 nm) but one can clearly notice in DMF the appearance of an

additional small band at 417 nm, attributed to the deprotonation of the phenol group in the ground state (D band). Excitation in this absorption band leads to the appearance of an intense D^* emission band at 467 nm but also to random aggregation processes as evidenced by a poor match between absorption and excitation spectra. As can been observed on Figure 5a, the absorption profile of HBO dye **6** in all solvents is slightly red-shifted as compared to **5** (λ_{abs} = 365-371 nm) but is not significantly influenced by the nature of the solvent except in DMF which leads to the appearance of an additional red-shifted absorption band (λ_{abs} = 460 nm) and an extra band at 361 nm as well. The lowest-energy band can be again assigned to the stabilization of the anionic species formed by deprotonation of the HBO dye **6** by DMF, the most basic of all solvents studied. Stabilization of related deprotonated HBO derivatives in DMF has already been observed and beneficially used for the engineering of white light emission.[19] In all solvents except DMF, HBO dye **6** exhibits a bright green/yellow emission upon photoexcitation at 350 nm with quantum yields in the range 21-35% (Figure 5c). Notably, the fluorescence efficiency remains high in the whole range of solvents studied, regardless of dipolarity or proticity. The K^* emission band maximum wavelength is not dependent on the nature of the solvent (λ_{em} = 540-550 nm). In DMF, however, upon photoexcitation in the lowest energy absorption band (λ_{em} = 450 nm), a distinctive intense blue emission is observed at 495 nm, attributed to the emission of the excited deprotonated species D^* (Figure 5c). The emission of the D^* state is stronger than that from the K^* state, as evidenced by a fluorescence quantum yield of 49%, calculated in DMF, the highest in the series for HBO dye **6**. It is important to note that unlike **5**, HBO **6** does not feature aggregates as evidenced by a good match between absorption and excitation spectra in DMF, evidencing the beneficial presence of the tertiobutyl group on the benzoxazole side but most importantly that of the ethynyl substitution at the 3-position of the phenol in order to enhance fluorescence intensity but also to decrease aggregation processes. The emission bands observed at 470 and 474 nm in THF and acetonitrile respectively are also assigned to the same D^* species. These photophysical processes are schematically summarized in Figure 6.

To ascertain the formation of the stabilized phenolate anion of HBO dye **6** in DMF, a large excess of potassium tert-butoxide (^{t}BuOK) was added and the optical properties recorded (Figure S3.12). No spectral difference can be observed in the absorption and emission profile of HBO dye **6**, upon addition of a large excess of base, further evidencing the intrinsic presence of the phenolate in both the ground and excited-states in DMF solution. It is noteworthy that the addition of an excess of hydrochloric acid in a DMF solution of HBO dye **6** leads to the appearance of a UV centered emission likely originating from the protonation of the benzoxazole ring.

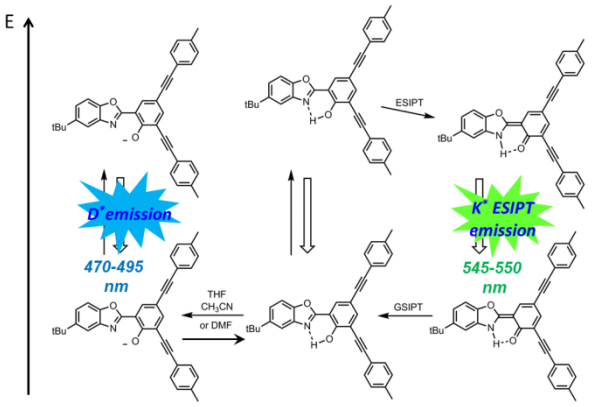

Figure 6. Simplified energy diagram showing the K^* emission (λ_{em} = 545-550 nm) stemming from the keto tautomer formed *via* ESIPT process and the D^* emission (λ_{em} = 470-495 nm) originating from deprotonation of the enol tautomer in the ground state, occurring partially or fully in DMF, THF and CH_3CN.

In order to investigate the formation and stability of the D^* band, absorption and emission titrations were performed on HBO dye **6** upon addition of increasing equivalent of a base, tetramethylammonium hydroxide (Me_4NOH) in acetonitrile (Figure 7).

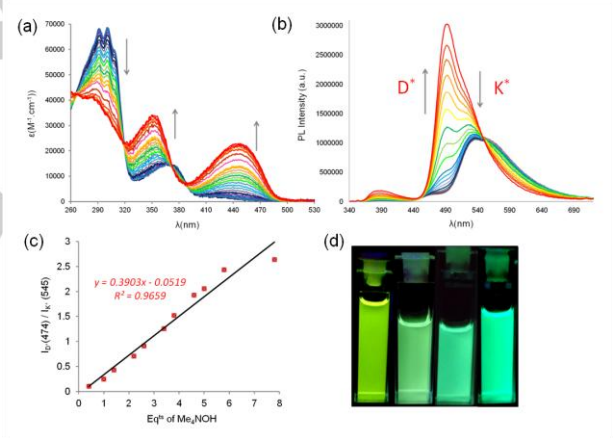

Figure 7. (a) Overlay of absorption spectra of HBO dye **6** in acetonitrile recorded after successive addition of increasing equivalents of Me_4NOH, (b) superposition of emission spectra, (c) plot of the ratio of intensity I(D^* at 474 nm)/I(K^* at 545 nm) *vs.* the number of added equivalents of Me_4NOH and (d) Photographs of acetonitrile solutions of HBO dye **6** under irradiation (λ_{exc} = 365 nm) before addition of base, after addition of two, five and ten equivalents (from left to right).

Acetonitrile was chosen as a solvent to ensure a good solubility of both HBO dyes **6** and Me_4NOH. In the absence of base, an absorption band with a maximum wavelength at 365 nm was recorded. Upon excitation at 360 nm, a dual emission profile was observed, consisting of a major band at 545 nm, assigned to the K^* tautomer and a minor (shoulder) band at 474 nm, attributed to the D^* form. Upon addition of increasing amounts of Me_4NOH, the absorption band at 365 nm was found to gradually decrease and lead to the appearance of

new bands at 352 nm and 446 nm, which is reminiscent of the absorption profile of fully deprotonated HBO dye **6** in DMF (λ_{abs} = 361/460 nm). In the successive recorded emission spectra, the fluorescence stemming from the D^* state at 474 nm rose, as a result of the deprotonation of HBO **6** while the K^* band at 545 nm showed a significant intensity decrease. Plotting the ratio of intensity of D^* (474 nm)/K^* (545 nm) *vs.* the number of base equivalents gives a good correlation (Figure 7c). The intensity ratio between the two emission bands D^*/K^* gradually increases upon addition of increasing amounts of base, until around 7 equivalents; after which a plateau is reached, corresponding to the full deprotonation of HBO **6**.

This gradual deprotonation of **6** in basic medium is also accompanied by the appearance of a small additional emission band at 388 nm which was also found in DMF in the absence of base. We assign the presence of this band to the minor formation of a benzofuran side-product obtained by an intramolecular cyclization in basic conditions.[14] To confirm the nature of this side-product whose *in situ* formation was observed during the titration, the synthesis of dye **13** was undertaken in one step from bis-iodo HBO derivative **11**. Without protection of the hydroxy group, Pd-catalyzed cross-coupling reaction between HBO **11** and p-tolyl acetylene in a mixture of toluene and triethylamine lead to the sole formation of dye **13** in 25% yield (Scheme 5).

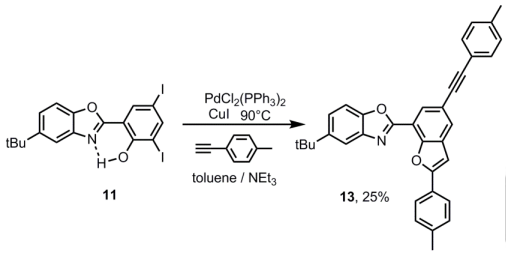

Scheme 5. Synthesis of dye **13**.

The photophysical data of compound **13** in acetonitrile are presented on Figure S3.13. A major absorption band at 300 nm is observed, along with an emission band at 390 nm upon photoexcitation, which corresponds to the emission wavelength of the side-product observed during the titration. This experiment further confirms the formation of compound **13** *in situ* during the basic titration. Unfortunately, the presence of this undesired compound impeded the accurate calculation of a pKa in the ground and excited state.

Outside their promising optical properties in solution, HBO dyes **1-6** appeared to be very bright as powders under irradiation at 365 nm by a bench UV-lamp by the naked eye (Figure 8b) which prompted us to investigate their photophysical behavior in the solid-state as dispersed in potassium bromide pellets. Their emission profiles appeared to be very similar to those observed in toluene, *i.e.* a single K^* emission band ranging from 489-547 nm depending on the position of substitution (Figure 8a). HBO dyes **3** and **6** bearing a mono- or disubstitution at the 5 or 3,5 position of the phenol ring respectively, are the most red-shifted in the series (λ_{em} = 530-547 nm for **3** and **6** *vs.* λ_{em} = 489-504 nm for all other dyes). Photoluminescent quantum yields, calculated as absolute using a spectrofluorimeter fitted with an integration sphere are significantly higher (Φ =48-88%) than those in solution; a feature encountered in the large majority of ESIPT emitters. HBO **1**, which was poorly emissive in the solution-state (Φ =4% in toluene) appears to be the brightest solid-state emitter in the series (Φ =88%).

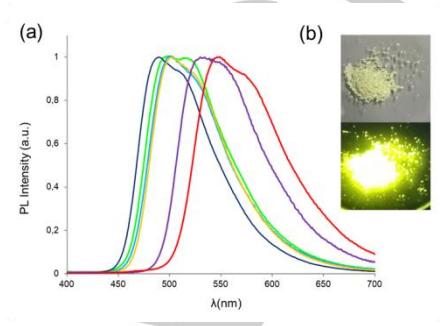

Figure 8. (a) Emission spectra recorded in KBr pellets at room temperature for HBO **1** (green), HBO **2** (navy blue), HBO **3** (pink), HBO **4** (light blue), HBO **5** (purple) and HBO **6** (red) and (b) Photographs of HBO **6** as a powder under daylight (top) and under irradiation with a bench UV lamp (λ_{exc} = 365 nm) (bottom).

To obtain complementary insights into the involved excited-state processes, *ab initio* calculations were performed following a protocol detailed in section S4. The results are collected in Table 2. The computed fluorescence wavelengths for the K^* emission in toluene very nicely match their experimental counterparts of Table 1, both quantitatively and qualitatively, with the most redshifted (blueshifted) emission observed for HBO dyes **5** and **6** (**1** and **4**), clearly confirming that this emission band originates from the keto form in the apolar solvent. This is further substantiated by computed driving forces for the ESIPT process ($\Delta G^{K^*-E^*}$) process that are all significantly negative indicating a favorable situation for proton transfer. The proton transfer is also computed to be barrierless by theory, with a transition state lying below the E^* form once entropic corrections are accounted for. Before analyzing the ethanol results, it should be recalled that the theoretical approach used for model solvent effects is a continuum model and therefore does not account for specific solute-solvent interactions but only for polarity effects. It turns out that the negative solvatochromism of the K^* band, evident from the measurements, is well reproduced by theory, so that this effect is probably mainly driven by the relative polarities of the excited states. In contrast, the computed ESIPT driving forces all remain strongly negative in the calculation, which is not in line with the emergence of dual emission experimentally observed in ethanol. One can therefore conclude that the frustration of the ESIPT process in ethanol is due to the formation of hydrogen bonds between the dye and the surrounding ethanol molecules.

Table 2. Theoretical data computed for dyes **1-6** in toluene and ethanol (DMF for **6**): emission wavelength and oscillator strengths determined for both the enol and keto tautomers, difference of free energy between the K^* and E^* forms, the ESIPT transition-state (TS-PT^*) and the E^* tautomer, and the twisting transition-state (TS-TW^*) and the K^* forms. See figure S3 in the SI for a representation of these key points. All values are obtained with TD-DFT and corrected with ADC(2), but the oscillator strength and twisting barrier that are the non-corrected TD-DFT results.

Dye	λ_{em} (E^*) (nm)	*f*	λ_{em} (K^*) (nm)	*f*	$\Delta G^{K^*-E^*}$ (eV)	$\Delta G^{TS-PT^*-E^*}$ (eV)	$\Delta G^{TS-TW^*-K^*}$ (eV)	Solvent
1	354	1.40	491	0.60	-0.25	-0.12	0.15	toluene
	358	1.55	481	0.74	-0.28	-0.11	0.00	EtOH
2	374	0.71	516	0.49	-0.28	-0.26	0.10	toluene
	382	1.00	505	0.66	-0.28	-0.26	0.06	EtOH
3	382	0.48	520	0.52	-0.20	-0.11	0.21	toluene
	384	0.73	511	0.65	-0.26	-0.12	0.02	EtOH
4	377	2.13	495	0.62	-0.15	-0.13	0.22	toluene
	382	2.33	489	0.84	-0.18	-0.07	0.11	EtOH
5	380	0.95	547	0.72	-0.28	-0.13	0.27	toluene
	376	1.27	528	0.89	-0.34	-0.14	0.09	EtOH
6	404	0.66	570	0.64	-0.27	-0.14	0.31	toluene
	404	0.85	555	0.77	-0.30	-0.13	0.06	DMF

As stated above, the fluorescence quantum yields in solution are generally limited by the presence of efficient non-radiative routes. Indeed, as can be seen in Table 2, all dyes present significant oscillator strengths, *i.e.* only very bright states are at play. For ESIPT dyes, one of the most well-known deactivating pathway is the twisting around the central interring bond after proton transfer (Figure S4.2.1), that can ultimately lead to a conical intersection with the ground state, and hence the emission quenching. To obtain first insights into that pathway, the transition state characterizing this twisting from the K^* tautomer was determined. As can be seen, positive barriers are systematically obtained, consistent with the presence of fluorescence. If one excludes HBO **2** in which the ethynyltolyl fragment is non-planar due to the interaction with the furan, it is noticeable in Table 2 that the largest barriers are determined for HBO dyes **5** (0.27 eV) and **6** (0.31 eV) in toluene, which are also the two compounds with the smallest K_{nr} (and largest Φ_F) of the series experimentally (Table 1). Conversely, the barriers for the twisting are very small for both dyes **2** and **5** in ethanol and these dyes indeed present very large K_{nr} and trifling Φ_F experimentally. This qualitative correlation therefore confirms that the twisting of the K^* tautomer is a relevant deactivation pathway, which is also consistent with the large increase of emission quantum yield in the solid state, where this large amplitude motion is hampered.

Finally, we have also modeled the anionic form of HBO **6** in DMF. Interestingly, our computational protocol predicts a bright emission (*f*=1.00) at 500 nm, that is in between the E^* and K^* band, which nicely fits the experimental value (495 nm), and therefore confirms the experimental assignment.

Conclusions

In summary, a series of ESIPT emitters based on ethynyl-tolyl-extended HBO scaffolds has been synthesized in a two-steps expedite synthesis. The photophysical properties were explored in multiple solvents where these dyes exhibit a single K^* or a dual E^*/K^* emission band with fluorescence quantum yield values reaching 35%. These values represent up to a 16-fold increase as compared to the unsubstituted reference dye, highlighting the beneficial introduction of these spacers on the molecular core. Depending on the position of the substitution, the stabilization of an anionic species was evidenced in a selection of dissociative solvents and by a basic titration in CH_3CN. These dyes keep their intense fluorescence emission in the solid-state, as embedded in KBr matrix, where a fine-tuning of the emission wavelength is observed. The nature of the excited-states was rationalized by *ab initio*. The origin of these enhanced optical properties is currently unclear but could be attributed to the restriction of the twisting around the central interring bond in the excited state. Transient absorption experiments along with time-resolved fluorescence spectroscopy are currently under investigation to shed more light on the excited-states dynamics in these systems.

Experimental Section

All reactions were performed under a dry atmosphere of argon. Chemicals were purchased from commercial sources and used without further purification. Reaction solvents were distilled according to common procedures. Thin layer chromatography (TLC) was performed on silica gel or aluminum oxide plates coated with fluorescent indicator. Chromatographic purifications were conducted using 40-63 µm silica gel. All mixtures of solvents are given in *v*/*v* ratio.

^{1}H NMR (400.1 MHz) and ^{13}C NMR (100.5 MHz) spectra were recorded on a Bruker Advance 400 MHz spectrometer, ^{1}H NMR (300.1 MHz) and ^{13}C NMR (75.5 MHz) on a Bruker Advance 300 MHz spectrometer with perdeuterated solvents containing residual protonated solvent signals as internal references.

Absorption spectra were recorded using a dual-beam grating Schimadzu UV-3000 absorption spectrometer with a 1 cm quartz cell. The steady-state fluorescence emission and excitation

spectra were obtained by using a Horiba S2 Jobin Yvon Fluoromax 4. All fluorescence spectra were corrected. Solvents for spectroscopy were spectroscopic grade and were used as received. All fluorescence spectra were corrected. The fluorescence quantum yield (Φ_{exp}) was calculated from eq (1).

$$\Phi_{\exp} = \Phi_{ref} \frac{I}{I_{ref}} \frac{OD_{ref}}{OD} \frac{\eta^2}{\eta^2_{ref}} \quad (\text{eq } 1)$$

I denotes the integral of the corrected emission spectrum, OD is the optical density at the excitation wavelength, and η is the refractive index of the medium. Quantum yield is determined in solution by using quinine sulfate as a reference (λ_{exc} = 366 nm, Φ = 0.55 in 1N H_2SO_4), for dyes emitting below 480 nm, Rhodamine 6G as a reference (λ_{exc} = 488 nm, Φ = 0.88 in ethanol), for dyes emitting between 480 and 570 nm or cresyl violet (λ_{exc} = 546 nm, Φ = 0.55 in ethanol) as a reference for dyes emitting above 570 nm. Solid-State emission was recorded using an integration sphere fitted to a spectrophotometer.

Luminescence lifetimes were measured on an Edinburgh Instruments spectrofluorimeter equipped with a R928 photomultiplier and a PicoQuant PDL 800-D pulsed diode connected to a GwInstect GFG- 8015G delay generator. No filter was used for the excitation. Emission wavelengths were selected by a monochromator. Lifetimes were deconvoluted with FS-900 software using a light-scattering solution (LUDOX) for instrument response. The excitation source was a laser diode (λ_{exc} = 320 nm). HBO **3**[13] and **4**[13] and salicylaldehyde **8**[20] were synthesized according to reported procedures.

General procedure for the synthesis of HBO dyes 7 and 10

The relevant salicylaldehyde (0.6 mmol) and 2-aminophenol derivatives (0.66 mmol, 1.1 equivalent), boronic acid (0.72 mmol., 1.2 equivalent) and potassium cyanide (1.8 mmol, 3 equivalents) were stirred overnight at room temperature in 40 mL of MeOH. The solvents were removed *in vacuo* and the crude mixture purified by column chromatography on SiO_2 (CH_2Cl_2/Pet. Ether. 1:9 to 2:8) to afford HBO dyes **7** and **10** as white powders.

HBO dye 7.65%. ^{1}H NMR (400MHz, $CDCl_3$) δ (ppm): 11.16 (s, 1H, OH), 7.99 (dd, 1H, CH, ^3J = 8Hz, ^4J = 1.6Hz), 7.86 (s, 1H, CH), 7.42-7.48 (m, 3H, CH), 7.10 (dd, 1H, CH, ^3J = 8.4Hz, ^4J = 0.7Hz), 7.00 (t, 1H, CH, ^3J = 8.3Hz). ^{13}C NMR (100.5Hz, $CDCl_3$) δ (ppm):164.0, 158.9, 148.2, 141.6, 134.1, 128.4, 127.2, 122.2, 119.7, 117.8, 117.6, 111.9, 110.1. ESI-HRMS: calcd for $C_{13}H_9BrNO_2$: 291.9792 (M+H), found 291.9781 (M+H). IR (*v*, cm^{-1}): 3093, 1627, 1586, 1541, 1460, 1444, 1426, 1263, 1251, 1234, 1158, 800, 752, 706, 687.

HBO dye 10. 54%. ^{1}H NMR (400MHz, $CDCl_3$) δ (ppm): 12.27 (s, 1H, OH), 8.01 (dd, 1H, CH, ^3J = 7.6Hz, ^4J = 1.6Hz), 7.73-7.78 (m, 1H, CH), 7.70 (dd, 1H, CH, ^3J = 7.6Hz, ^4J = 1.6Hz), 7.60-7.65 (m, 1H, CH), 7.39-7.44 (m, 2H, CH), 6.93 (t, 1H, CH, ^3J = 8Hz). ^{13}C NMR (100.5Hz, $CDCl_3$) δ (ppm): 162.3, 155.6, 149.5, 139.8, 137.0, 126.5, 126.1, 125.5, 120.6, 119.7, 111.9, 111.5, 111.0. ESI-HRMS: calcd for $C_{13}H_9BrNO_2$: 291.9792 (M+H), found 291.9775 (M+H). IR (*v*, cm^{-1}): 2869, 1628, 1579, 1543, 1452, 1402, 1343, 1289, 1241, 1146, 1071, 813, 758, 747, 736.

General procedure for the synthesis of HBO dyes 9 and 11

To a solution of 2-aminophenol or 4-tertiobutyl-2-aminophenol (0.5 mmol) in absolute ethanol was added salicylaldehyde **8** or 3,5-diiodo-2-hydroxybenzaldehyde (0.5 mmol) and the resulting suspension was refluxed for one hour before an orange precipitate formed. After cooling down, the precipitate was filtered and washed with ethanol. It was then redissolved in dry dichloromethane and 2,3-dichloro-5,6-dicyano-1,4-benzoquinone (DDQ) (0.6 mmol) was added as a concentrated dichloromethane solution. The resulting dark mixture was stirred at room temperature overnight. After solvent evaporation, the crude residue was purified by silica gel chromatography eluting with CH_2Cl_2/Pet. Ether 1:2 leading to HBO **9** or **11** as a white powders.

HBO dye 9. 57%. ^{1}H NMR (400MHz, $CDCl_3$) δ (ppm): 12.60 (s, 1H, OH), 7.74-7.78 (m, 1H, CH), 7.68-7.72 (m, 1H, CH), 7.66 (dd, 1H, CH, ^3J = 7.6Hz, ^4J = 1.2Hz), 7.41-7.46 (m, 2H, CH),), 7.12 (dd, 1H, CH, ^3J = 8.4Hz, ^4J = 1.2Hz), 7.03 (t, 1H, CH, ^3J = 8Hz). ^{13}C NMR (100.5Hz, $CDCl_3$) δ (ppm): 161.4, 160.8, 148.7, 138.8, 133.8, 133.5, 125.9, 125.4, 119.2, 117.9, 114.2, 111.1, 91.2. ESI-HRMS: calcd for $C_{13}H_9INO_2$: 337.9673 (M+H), found 337.9663 (M+H). IR (*v*, cm^{-1}): 1617, 1572, 1522, 1445, 1310, 1281, 1176, 1085, 1041, 1002, 948, 770, 748, 735.

HBO dye 11. 75%. ^{1}H NMR (400MHz, $CDCl_3$) δ (ppm): 12.45 (s, 1H, OH), 8.27 (s, 1H, CH), 8.14 (s, 1H, CH), 7.72 (s, 1H, CH), 7.46-7.52 (m, 2H, CH), 1.39 (s, 9H, CH_3). ^{13}C NMR (100.5Hz, $CDCl_3$) δ (ppm): 160.5, 157.2, 149.5, 149.2, 147.4, 139.3, 135.3, 124.1, 116.0, 112.5, 110.1, 86.7, 81.0, 35.1, 31.8. ESI-HRMS: calcd for $C_{17}H_{16}I_2NO_2$: 519.9186 (M+H), found 519.9117 (M+H). IR (*v*, cm^{-1}): 3066, 2955, 1600, 1568, 1532, 1483, 1426, 1411, 1334, 1274, 1249, 1176, 1126, 1065, 936, 854, 812, 760, 649.

Synthesis of HBO dye 1

Halogenated HBO dye **7** (0.5 mmol.), p-tolylacetylene (1.5 mmol.) and $Pd(dppf)Cl_2$ (5 % molar) were dissolved in 25 mL of toluene/triethylamine (3/1 *v:v*). The resulting suspension was degassed with argon for 30 minutes before CuI (10 % molar) was added. The resulting mixture was stirred overnight at 90°C. The dark solution was taken up in dichloromethane, washed with water, dried ($MgSO_4$) and concentrated *in vacuo*. The product was purified by silica gel chromatography (CH_2Cl_2/Pet. Ether 1:3 to 1:1) to afford clean HBO dyes **1** as a white powder. 37%. ^{1}H NMR (400MHz, $CDCl_3$) δ (ppm): 11.33 (s, 1H, OH), 8.00 (dd, 1H, CH, ^3J = 7.9Hz, ^4J = 1.6Hz), 7.87 (s, 1H, CH), 7.52-7.57 (m, 2H, CH), 7.42-7.46 (m, 3H, CH), 7.16 (d, 2H, ^3J = 7.9Hz), 7.12 (d, 1H, ^3J = 7.9Hz), 7.00 (t, 1H, CH), 2.37 (s, 3H, CH_3). ^{13}C NMR (100.5Hz, $CDCl_3$) δ (ppm): 164.0, 159.1, 149.1, 140.4, 138.8, 134.1, 131.7, 129.4, 129.4, 127.4, 122.5, 120.8, 120.2, 119.9, 117.7, 110.9, 110.5, 89.6, 88.3, 21.8. ESI-HRMS: calcd for $C_{22}H_{16}NO_2$: 326.1176 (M+H), found 326.1163 (M+H). IR (*v*, cm^{-1}): 3027, 1631, 1586, 1513, 1486, 1464, 1428, 1296, 1252, 1224, 1192, 1053, 934, 809, 754, 719.

Synthesis of HBO dye 2

Halogenated HBO dye **9** (0.5 mmol.), p-tolylacetylene (1.5 mmol.) and $Pd(PPh_3)_2Cl_2$ (5 % molar) were dissolved in 25 mL of toluene/triethylamine (3/1 *v:v*). The resulting suspension was degassed with argon for 30 minutes before CuI (10 % molar) was added. The resulting mixture was stirred overnight at 90°C. The dark solution was taken up in dichloromethane, washed with water, dried ($MgSO_4$) and concentrated *in vacuo*. The product

was purified by silica gel chromatography (CH_2Cl_2/Pet. Ether 1:3 to 1:1) to afford clean HBO dye **2** as a white powder. 67%. ^{1}H NMR (400MHz, $CDCl_3$) δ (ppm): 12.54 (s, 1H, OH), 7.75-7.79 (m, 1H, CH), 7.61-7.65 (m, 1H, CH), 7.56 (d, 2H, CH, ^3J = 8Hz), 7.36-7.44 (m, 3H, CH), 7.23-7.26 (m, 3H, CH), 7.11 (dd, 1H, CH, ^3J = 8Hz, ^4J = 1.2Hz), 2.42 (s, 3H, CH_3). ^{13}C NMR (100.5Hz, $CDCl_3$) δ (ppm): 163.0, 159.7, 149.1, 139.0, 138.9, 132.4, 132.3, 131.4, 129.3, 125.6, 125.2, 122.5, 120.5, 119.2, 117.7, 111.0, 110.8, 94.2, 88.4, 21.7. ESI-HRMS: calcd for $C_{22}H_{16}NO_2$: 326.1176 (M+H), found 326.1191 (M+H). IR (*v*, cm^{-1}): 2910, 2850, 1615, 1597, 1573, 1510, 1451, 1245, 1175, 1048, 995, 816, 733.

General procedure for the synthesis of HBO dyes 5 and 6

Halogenated HBO dyes **10** or **11** (0.5 mmol.), were dissolved in 20 mL of dichloromethane. 8 mL of acetic anhydride and 2 mL of pyridine were then added and the mixture stirred at room temperature for 3 hours. The crude solution was then diluted with 50 mL of dichloromethane, washed with HCl 0.1M and water, dried ($MgSO_4$) and the solvents evaporated *in vacuo*. The resulting oil was dissolved in 25 mL of toluene/triethylamine (3/1 *v:v*). p-tolylacetylene (1.5 mmol.) and $Pd(PPh_3)_2Cl_2$ or $Pd(dppf)Cl_2$ (5 % molar) were then added and the resulting suspension was degassed with argon for 30 minutes before CuI (10 % molar) was added. The resulting mixture was stirred overnight at 90°C. The dark solution was taken up in dichloromethane, washed with water, dried ($MgSO_4$) and concentrated *in vacuo*. The product was purified by silica gel chromatography (CH_2Cl_2/Pet. Ether 1:3 to 1:1) to afford clean HBO dyes **5** or **6** as white powders.

HBO dye 5. 20%. ^{1}H NMR (400MHz, $CDCl_3$) δ (ppm): 12.12 (s, 1H, OH), 7.99 (dd, 1H, CH, ^3J = 8 Hz, ^4J = 1.7Hz), 7.70-7.75 (m, 1H, CH), 7.58-7.64 (m, 2H, CH), 7.49 (d, 2H, CH, ^3J = 8.1 Hz), 7.36-7.41 (m, 2H, CH), 7.16 (d, 2H, CH, ^3J = 7.8Hz), 6.99 (t, 1H, CH, ^3J = 7.8Hz), 2.36 (s, 3H, CH_3). ^{13}C NMR (100.5Hz, $CDCl_3$) δ (ppm): 162.7, 159.4, 149.4, 140.0, 138.7, 137.0, 131.9, 129.3, 127.2, 125.8, 125.3, 120.5, 119.6, 119.5, 113.1, 111.0, 110.9, 94.8, 84.3, 21.8. ESI-HRMS: calcd for $C_{36}H_{29}NO_2$: 326.1176 (M+H), found 326.1170 (M+H). IR (*v*, cm^{-1}): 2918, 2850, 1622, 1589, 1541, 1451, 1416, 1259, 1244, 1119, 1099, 812, 756, 744, 731.

HBO dye 6. 90%. ^{1}H NMR (400MHz, $CDCl_3$) δ (ppm): 12.31 (s, 1H, OH), 8.16 (d, 1H, CH, ^4J = 2 Hz), 7.78 (d, 1H, CH, ^4J = 2 Hz), 7.74 (d, 1H, CH, ^4J = 1.4 Hz), 7.44-7.54 (m, 4H, CH), 7.42 (d, 2H, CH, ^4J = 8.1 Hz), 7.16 (dd, 4H, CH, ^3J = 7.7 Hz, ^4J = 2.7 Hz), 2.37 (s, 6H, CH_3), 1.40 (s, 9H, CH_3). ^{13}C NMR (100.5Hz, $CDCl_3$) δ (ppm): 162.2, 159.0, 149.2, 147.5, 139.9, 139.5, 138.9, 138.7, 131.9, 131.7, 130.1, 129.4, 129.3, 123.9, 120.3, 116.2, 115.1, 113.6, 111.4, 110.2, 95.2, 89.1, 87.4, 83.6, 35.3, 32.0, 21.8, 21.8. ESI-HRMS: calcd for $C_{22}H_{16}NO_2$: 496.2271 (M+H), found 496.2280 (M+H). IR (*v*, cm^{-1}): 2961, 2864, 1596, 1546, 1508, 1479, 1440, 1394, 1303, 1267, 1252, 1224, 872, 809, 766.

Synthesis of dye 13

HBO dye **11** (0.5 mmol.) was dissolved in 25 mL of toluene/triethylamine (3/1 *v:v*). p-tolylacetylene (1.5 mmol.) and $Pd(PPh_3)_2Cl_2$ (5 % molar) were then added and the resulting suspension was degassed with argon for 30 minutes before CuI (10 % molar) was added. The resulting mixture was stirred overnight at 90°C. The dark crude was taken up in dichloromethane, washed with water, dried ($MgSO_4$) and concentrated *in vacuo*. The product was purified by silica gel chromatography (CH_2Cl_2/Pet. Ether 1:3) to afford clean dye **13** as a white powder in 25% yield. ^{1}H NMR (400MHz, $CDCl_3$) δ (ppm): 8.33 (d, 1H, CH, ^4J = 1.6 Hz), 7.85-7.90 (m, 4H, CH), 7.58 (d, 1H, CH, ^3J = 6.8 Hz), 7.44-7.47 (m, 3H), 7.30 (d, 2H, CH, ^3J = 6.4 Hz), 7.17 (d, 2H, CH, ^3J = 6.4 Hz), 7.02 (s, 1H, CH), 2.42 (s, 3H, CH_3), 2.37 (s, 3H, CH_3), 1.42 (s, 9H, CH_3). ^{13}C NMR (100.5Hz, $CDCl_3$) δ (ppm): 160.0, 158.5, 151.3, 148.8, 148.2, 142.1, 139.4, 138.5, 131.5, 131.4, 129.6, 129.2, 127.7, 127.0, 126.5, 125.4, 123.2, 120.2, 118.8, 116.9, 112.2, 110.0, 100.2, 89.0, 88.2, 35.0, 31.9, 21.5. ESI-HRMS: calcd for $C_{35}H_{30}NO_2$: 496.2271 (M+H), found 496.2278 (M+H).

Acknowledgments

J.M. and G.U. thank the Centre National de la Recherche Scientifique (CNRS), the Agence Nationale de la Recherche (ANR) (GeDeMi grant) and the SATT Conectus (Dualem maturation project) for funding. M.M. thanks the Région Alsace and *Amoneta Diagnostics* for funding of a Ph.D. grant.

Keywords: Fluorescence • Hydroxybenzazole • ESIPT • TD-DFT calculations

[1] Special issue "Photoinduced Proton Transfer in Chemistry and Biology", *J. Phys. Chem B* **2015**, 119, 2089-2768.

[2] (a) G. Granucci, J.T. Hynes, P. Millié, T.-H. Tran-Thi, *J. Am. Chem. Soc.* **2000**, 122, 12243-12253. (b) J. Zhao, S. Ji, Y. Chen, H. Guo, P. Yang, P. *Phys. Chem. Chem. Phys*. **2012**, 14, 8803-8817.

[3] (a) A. Weller, *Z. Elektrochem*. **1956**, 60, 1144-1147. (b) J. Goodman, L.E. Brus, J. *Am. Chem. Soc*. **1978**, 100, 7472-7474.

[4] (a) M. Ikegami, T. Arai, *J. Chem. Soc., Perkin Trans*. **2002**, 2, 1296-1301. (b) K. Benelhadj, W. Muzuzu, J. Massue, P. Retailleau, A. Charaf-Eddin, A.D. Laurent, D. Jacquemin, G. Ulrich, R. Ziessel, *Chem. Eur. J*. **2014**, 20, 12843-12857. (c) E. Heyer, K. Benelhadj, S. Budzák, D. Jacquemin, J. Massue, G. Ulrich, *Chem. Eur. J*. **2017**, 23, 7324-7336. (d) D. Yao, S. Zhao, J. Gao, Z. Zhang, H. Zhang, Y. Liu, Y. Wang, *J. Mater. Chem*. **2011**, 21, 3568-3570. (e) K. Benelhadj, J. Massue, G. Ulrich, G.; *New. J. Chem*. **2016**, 40, 5877-5884.

[5] (a) G. Ulrich, F. Nastasi, P. Retailleau, F. Puntoriero, R. Ziessel, S. Campagna, *Chem. Eur. J*. **2008**, 14, 4381-4392. (b) A.J. Stasuyk, M. Banasiewicz, B. Ventura, M.K. Cyranski, D.T. Gryko, *New. J. Chem*. **2014**, 38, 189-197. (c) K. Skonieczny, A.I. Ciuciu, E.M. Nichols, V. Hugues, M. Blanchard-Desce, L. Flamigni, D.T. Gryko, *J. Mater. Chem*. **2012**, 22, 20649-20664. (d) A.J. Stasyuk, M. Banasiewicz, M.K. Cyranski, D.T. Gryko, *J. Org. Chem*. **2012**, 77, 5552-5558.

[6] (a) Y.-H. Hsu, Y.-A. Chen, H.-W. Tseng, Z. Zhang, J.-Y. Shen, W.-T. Chuang, T.-C. Lin, C.-S. Lee, W.-Y. Hung, B.-C. Hong, S.-H. Liu, P.-T. Chou, *J. Am. Chem. Soc*. **2014**, 136, 11805-11821. (b) F.-Y. Meng, Y.-H. Hsu, Z. Zhang, P.-J. Wu, Y.-T. Chen, Y.-A. Chen, C.-L. Chen, C.-M. Chao, K.-M. Liu, P.-T. Chou, *Chem. Asian J*. **2017**, 12, 3010-3015. (c) T. Iijima, A. Momotake, Y. Shinohara, T. Sato, Y. Nishimura, T. Arai, *J. Phys. Chem. A* **2010**, 114, 1603-1609. (d) J. Li, Y. Wu, Z. Xu, Q. Liao, H. Zhang, Y. Zhang, L. Xiao, J. Yao, H. Fu, *J. Mater. Chem C* **2017**, 5, 12235-12240.

[7] (a) J. Massue, D. Jacquemin, G. Ulrich, *Chem. Lett*., **2018**, 47, 1083-1089. (b) C. Azarias, S. Budzák, A.D. Laurent, G. Ulrich, D. Jacquemin, *Chem. Sci*. **2016**, 7, 3763-3774.

[8] A. Klymchenko, *Acc. Chem. Res*. **2017**, 50, 366-375.

[9] M. Sholokh, O.M. Zamotaiev, R. Das, V.Y. Postupalenko, L. Richert, D. Dujardin, O.A. Zaporozhets, V.G. Pivovarenko, A.S. Klymchenko, Y. Mely, *J. Phys. Chem. B* **2015**, 119, 2585-2595.

[10] (a) W.-H. Chen, Y. Pang, *Org. Lett*. **2011**, 13, 1362-1365; (d) S. Goswami, S. Das, K. Aich, B. Pakhira, S. Panja, W-H. Mukherjee, S. Sarkar, *Org. Lett*. **2013**, 15, 5412-5415.

[11] V.S. Padalkar, S. Seki, *Chem. Soc. Rev*. **2016**, 45, 169-202.

[12] (a) K. Skonieczny, J. Yoo, J.M. Larsen, E.M. Espinoza, M. Barbasiewicz, V.I. Vullev, C.-H. Lee, D.-T. Gryko, *Chem. Eur. J.* **2016**, 22, 7485-7496. (b) K. Takagi, K. Ito, Y. Yamada, T. Nakashima, R. Fukuda, M. Ehara, H. Masu, *J. Org. Chem*. **2017**, 82, 12173-12180. (c) N. Suzuki, A. Fukazawa, K. Nagura, S. Saito, H. Kitoh-Nishioka, S. Irle, D. Yokogawa, S. Yamaguchi, *Angew. Chem., Int. Ed.*, **2014**, 53, 8231-8235; *Angew. Chem*. **2014**, 126, 8370-8374. (d) N. Suzuki, K. Suda, D. Yokogawa, H. Kitoh-Nishioka, S. Irle, A. Ando, L.M.G. Abegao, K. Kamada, A. Fukazawa, S. Yamaguchi, *Chem. Sci*. **2018**, 9, 2666-2673.

[13] J. Massue, D. Frath, P. Retailleau, G. Ulrich, R. Ziessel, *Chem. Eur. J*. **2013**, 19, 5375-5386.

[14] (a) Y.-Y. Sun, J.-H. Liao, J.-M. Fang, P.-T. Chou, C.-H. Shen, C.-W. Hsu, L.-C. Chen, *Org. Lett*. **2006**, 8, 3713–3716. (b) K. Benelhadj, M. Munch, J. Massue, G. Ulrich, *Tetrahedron*, **2016**, 72, 2593-2599.

[15] G. Yang, K. Zhang, F. Gong, M. Liu, Z. Yang, J. Ma, S. Li, *Sensors and Actuators B* **2011**, 155, 848-853.

[16] Q. Wang, L. Xu, Y. Niu, Y. Wang, M.-S. Yuan, Y. Zhang, *Chem. Asian J*. **2016**, 11, 3454-3464.

[17] (a) A. Karpfen, *Adv. Chem. Phys*. **2002**, 123, 469-510. (b) Y. Peng, Y. Ye, X. Xiu, S. Sun, *J. Phys. Chem. A* **2017**, 121, 5625-5634.

[18] J. Cheng, D. Liu, W. Li, L. Bao, K. Han, *J. Phys. Chem C* **2015**, 119, 4242-4251.

[19] K.-I., Sakai, T. Ishikawa, T. Akutagawa, *J. Mater. Chem. C* **2013**, 1, 7866-7871.

[20] S M. Geddis, C.E. Hagerman, W.R.J.D. Galloway, H.F. Sore, J.M. Goodman, D.R. Spring, *Beilstein J. Org. Chem.* **2017**, 13, 323-328.

…

Entry for the Table of Contents

FULL PAPER

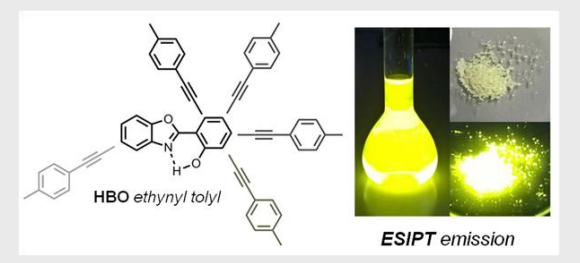

A series of ESIPT emitters based on ethynyl-extended HBO scaffolds has been synthesized. Their optical properties reveal increased quantum yields values in solution as compared to unsubstituted analogues while keeping strong fluorescence intensities in the solid-state. These scaffolds also allow the stabilization of an anionic species in selected cases, as evidenced by basic titrations. The nature of the excited-states was also rationalized using *ab initio* calculations.

Maxime Munch, Mathieu Curtil, Pauline M. Vérité, Denis Jacquemin, Julien Massue[a]* and Gilles Ulrich**

Page No. – Page No.

Ethynyl-Tolyl Extended 2-(2'-Hydroxyphenyl)benzoxazole Dyes as Optimized Solution and Solid-state Excited-State Intramolecular Proton Transfer (ESIPT) Emitters